2024, 21(3): 0952-0961
https://dx.doi.org/10.21123/bsj.2023.8183
P-ISSN: 2078-8665 - E-ISSN: 2411-7986
Baghdad Science Journal

Biosynthesis, Characterization, Adsorption and Antimicrobial studies of Manganese oxide Nanoparticles Using Punica Granatum Extract

Angham Tariq Ali , ***Lekaa K. Abdul Karem*** *

Department of Chemistry, College of Education for Pure Sciences (Ibn Al-Haitham), University of Baghdad, Baghdad, Iraq.
*Corresponding Author.

Received 29/11/2022, Revised 25/02/2023, Accepted 27/02/2023, Published Online First 20/08/2023, Published 01/03/2024

Abstract

Manganese sulfate and Punica granatum plant extract were used to create MnO_2 nanoparticles, which were then characterized using techniques like Fourier transform infrared spectroscopy, ultraviolet-visible spectroscopy, atomic force microscopy, X-ray diffraction, transmission electron microscopy, scanning electron microscopy, and energy-dispersive X-ray spectroscopy. The crystal's size was calculated to be 30.94nm by employing the Debye Scherrer equation in X-ray diffraction. MnO_2 NPs were shown to be effective in adsorbing M(II) = Co, Ni, and Cu ions, proving that all three metal ions may be removed from water in one go. Ni(II) has a higher adsorption rate throughout the board. Co, Ni, and Cu ion removal efficiencies were 32.79%, 75.00%, and 30.20%, respectively. Two species of bacteria and one type of fungus were examined at three different use concentrations if possible of MnO_2 nanoparticles. Antibiotics like Amoxicillin and Metronidazole were used as a control group to see how the findings stacked up.

Keywords: Adsorption, Antimicrobial, Biosynthesis, Manganese oxide, Removal.

Introduction

Nanotechnology is a burgeoning area of study in medicine. It is the responsibility of nanoparticles, an intermediary between micro materials and atomic structures, to improve the physical qualities such as surface area and volume ratio [1]. The development of novel medications has used the therapeutic characteristics that herbal plants and their derivatives contain [2]. MnO_2 has attracted the attention of numerous researchers due to its impact and electromagnetic properties [3]. MnO_2 has been synthesized using various techniques, including self-reacting microemulsion, deposition, and solid reaction [4]. However, using natural compounds to decrease and stabilize Mn metal into nanoparticles is more environmentally friendly, less expensive, and more straightforward than the preceding procedures [5]. Escherichia coli, Klebsiella pneumonia, and Pseudomonas aeruginosa are pathogenic microorganisms that can harm individuals with weakened natural defenses and result in severe systemic disease [6]. Due to their nanoscale size, NPs can penetrate biofilms and bacterial cell walls and have a cytotoxic effect. They can also increase the effectiveness of current

2024, 21(3): 0952-0961
https://dx.doi.org/10.21123/bsj.2023.8183
P-ISSN: 2078-8665 - E-ISSN: 2411-7986
Baghdad Science Journal

antibiotics by preventing their detection and providing a method of targeted delivery to microorganisms to maximize their topical concentration and bactericidal effects [7]. In this study, we sought to synthesize MnO_2 NPs using Punica Granatum extract as the reducing and capping agents, characterize the synthesized MnO_2 NPs, and assess their antibacterial effectiveness versus bacteria, both on their own and in combination with other antibiotics.

Materials and Methods

Obtaining samples Punica granatum was gathered and marked from a nearby source, and we used hydrated manganese sulfate. $MnSO_4.H_2O$ was purchased from England, NaOH from Alpha India's Alpha Chemical, ethanol from Samka Aldaraj, and copper, cobalt, and nickel sulfate. Several spectroscopic and microscopic methods were used to make and identify the compounds, including the following: a magnetic stirrer, a sensitive **electronic balance** model As 220C1, a centrifuge type PLC, and an **electric oven** type (FAITHFUL) model - WHL. And an **XRD diffraction** type PW1730 (Phillips/ Holland). Shaking Water Bath type (SCL FINETEDI), PH-type **UV-visible** tape measure (160/Uv) Shimadzu using the deionized water as a solvent, **FT-IR** (8500S) type spectroscopy in 400-4000 cm^{-1}, and (centre of examinations). Application of an X-ray energy dispersion device, **SEM** type FESEM-EDS Model MIRAIII, manufacturer TESCAN, and country of manufacture Czech (**EDX**). **TEM** with the EM10C-100Kv model number and Atomic Force Microscopes **AFM**.

Preparation of Punica Granatum extract and MnO_2 NPs

Deionized water has been used to wash the fresh pomegranate peel and eliminate dust. To create homogeneous powders, the dry pomegranate peel is carefully blended in a mixer. After that, 20 g were ground up and combined with 200 ml of deionized water. The mixture was heated for 30 minutes at 60 °C while being stirred. After filtering, the solution was placed in the refrigerator. From the preparation of MnO_2, NPs were created using the green synthesis method. As a result, 0.1M, 50 ml of $MnSO_4.H_2O$, and 100 ml of pomegranate peel extract were added slowly (one drop per second) and stirred for 30 minutes. The solution was then given 40 ml of 1 N NaOH. The pH level rose to 10-12. The result was a dark black crystal precipitate cleaned with deionized water (all steps were done with centrifuge and then decantation). They were dried for 4 hours at 120 °C before being dried again for 4 hours at 250 °C. Manganese oxide nanoparticles were produced as a black powder.

Adsorption study

To create a stock solution, 10g of $CoCl_2.6H_2O$ were dissolved in one litre of distilled water to produce 10000 ppm. The stock concentration for $NiCl_2.4H_2O$ and $CuCl_2.2H_2O$ was 5000 ppm because the stock was made by dissolving 5g in 1 litre of distilled water.

Adsorption of metal ions on the surface of MnO_2 NPs was performed by adding 0.1 g of the adsorbent nanoparticle to 50 ml of a 1000 ppm metal ion solution in a shaker water bath at 26 ºC and shaking at 150 revolutions per minute (rpm). The adsorbent was then separated from the solution at specific times by centrifuging. A visible spectrophotometer measured the remaining clear solution to determine the remaining concentration after adsorption using the calibration curve

Biological Activity Study

Using the disc diffusion method in a nutrient medium (jellos medium) type Muller Hinton agar, the antimicrobial activity of the synthetic MnO_2 NPs in concentrations of about (25, 50, and 75) mg/L, was tested against two reference bacterial strains (G+) Staphylococcus aurous, and (G-), Escherichia coli, and the fungus Candida albicans. Likewise, the antifungal activity of a nutrient medium based on potato dextrose was measured using the same method.

2024, 21(3): 0952-0961
https://dx.doi.org/10.21123/bsj.2023.8183
P-ISSN: 2078-8665 - E-ISSN: 2411-7986
Baghdad Science Journal

Results and Discussion

FT-IR analysis

The FTIR of MnO_2 shows in Fig. 1, bands at 590 and 532 cm^{-1} in the FTIR spectra of MnO_2 are attributed to the Mn-O stretching mode, proving the presence of the Mn-O bond in the MnO_2 structure [8, 9]. Absorption bands at 1643.35, 1411.89, and 1554.83 cm^{-1} stretching correspond to O-H bending vibrations linked with Mn atoms. In contrast, the absorption band at 3425.58 cm^{-1} arises from varying degrees of hydrogen bonding within the sample. O-H vibrations in the FTIR spectrum, were observed, and are indicative of water molecules being absorbed into the MnO_2 structure.

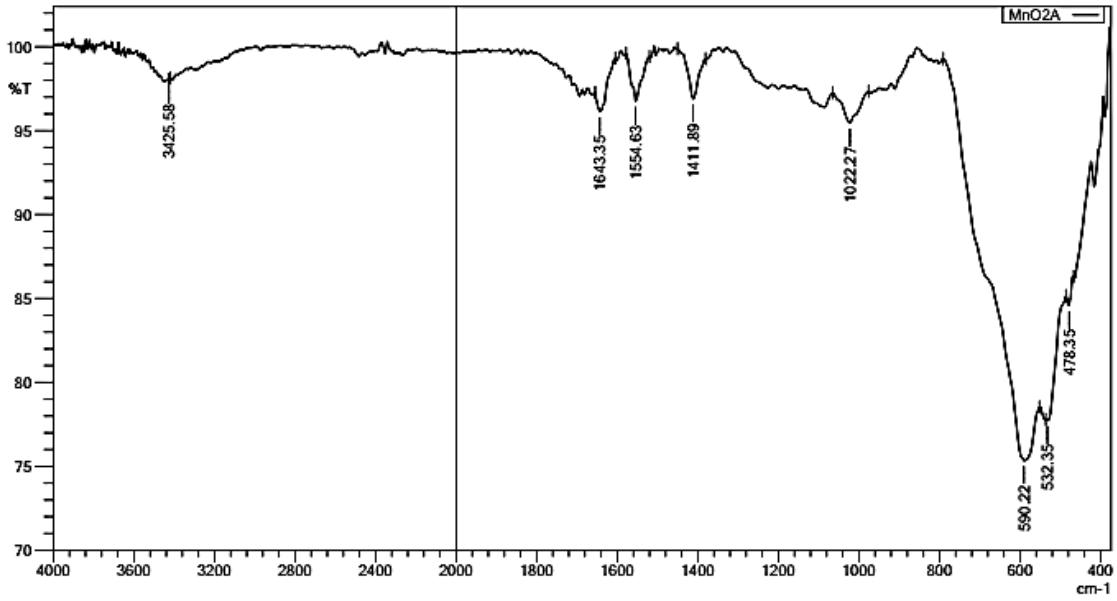

Figure 1. FT-IR spectrum of MnO_2 NPs

UV-Visible analysis

The UV-Vis absorption spectrum of the biosynthesis of MnO_2 NPs is shown in Fig. 2. The absorption peak in this spectrum at 348.0 nm was due to the transition holes process between Mn and O.

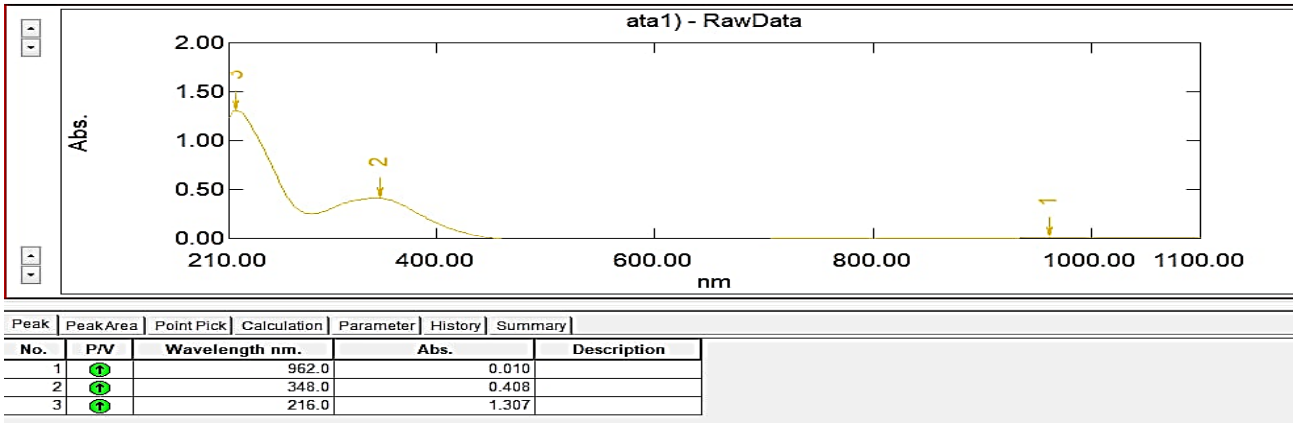

Figure 2. UV-Visible spectrum of MnO_2NPs

XRD analysis

According to XRD analysis, orthorhombic MnO_2 consistent with 110, 200, 310, 201, 301, 500 and 451 crystal planes are allocated to a series of diffraction peaks at 2θ of 12.8657, 18.2382, 28.8139, 37.5886, 42.0775, 43.1011, 49.9468,

2024, 21(3): 0952-0961
https://dx.doi.org/10.21123/bsj.2023.8183
P-ISSN: 2078-8665 - E-ISSN: 2411-7986
Baghdad Science Journal

56.8433, 59.6661 and 72.8652, respectively, JCPDS card (no. 44–0141). XRD measurements, which showed no impurity peaks, are evidence that MnO_2 NPs samples are highly crystalline. The average crystal size was calculated using the Debye Scherrer equation ($D = 0.9\ \lambda / \beta \cos\theta$) where D= the average crystalline size, the Cu K X-ray radiation (λ = 1.5418 ºA), was discovered to be 35.74nm in Fig. 3 and Table 1.

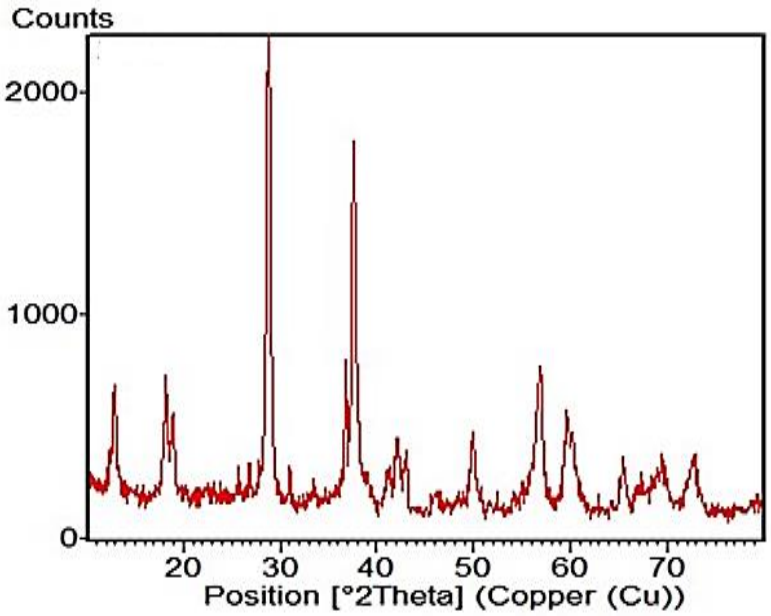

Figure 3. XRD of MnO_2 NPs

Table 1. The data of XRD for MnO_2 Nps.

Pos. [°2Th.]	Height [cts]	FWHM [°2Th.]	Particle size (nm)	Average crystal size (nm)
12.8657	519.51	0.246	33.97	
18.2382	525.75	0.1476	56.98	
28.8139	2023.78	0.3444	24.89	
37.5886	1472.47	0.2952	29.71	30.94
42.0775	309.71	0.3936	22.60	
43.1011	181.99	0.246	36.29	
49.9468	318.60	0.3936	23.27	
56.8433	646.58	0.1968	47.98	
59.6661	421.39	0.492	19.46	
72.8652	220.68	0.72	14.33	

EDX analysis

The EDX spectrum of MnO_2 Nps shows the expected peaks for manganese and oxygen. Having a 1:1 ratio between them Fig. 4. The results demonstrate how exceptionally pure the generated nanoparticles are—the outcomes of the EDX measurement's accurate estimations and fundamental theoretical calculations also agree[9].

2024, 21(3): 0952-0961
https://dx.doi.org/10.21123/bsj.2023.8183
P-ISSN: 2078-8665 - E-ISSN: 2411-7986
Baghdad Science Journal

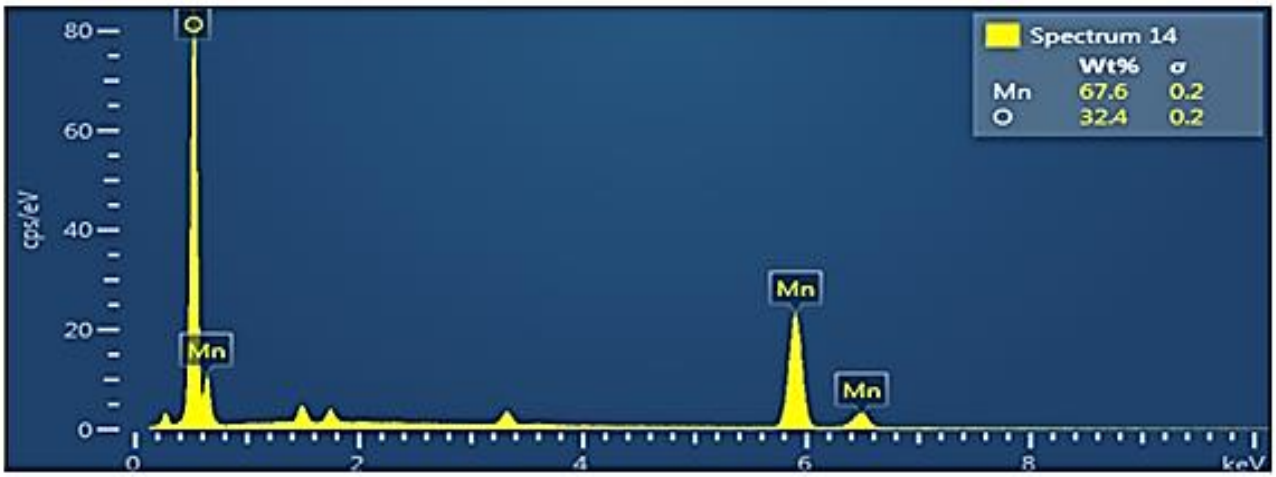

Figure 4. EDX of MnO_2 Nps.

SEM and TEM analysis

SEM and TEM were used to determine the Morphology and shapes of nanomaterials. Low amounts of rods in nanostructured, unconsolidated forms of MnO_2 NPs can be seen in SEM and TEM measurements of Figs. 5 and 6. In the TEM picture, the MnO_2 nanoparticles emerged as UN-consolidated structures at the nanoscale. It should also be highlighted that the samples exhibit high pore content, which distinguishes them in adsorption applications. The shape of Mno_2 nanoparticles was found to be packed together in the TEM image. Due to the accuracy of the measurement, the sample's shape cannot be determined with absolute certainty, but it appears to contain measurements of the sample's spherical internal structure that are zero-dimensional (all of its dimensions are nanoscale), which is highly preferred in surface chemistry for nanomaterial's[10].

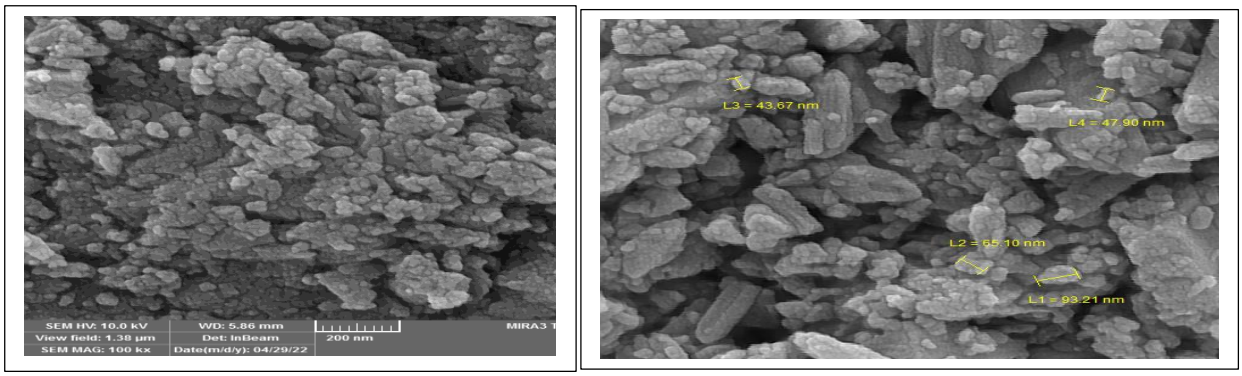

Figure 5. SEM of MnO_2 NPs.

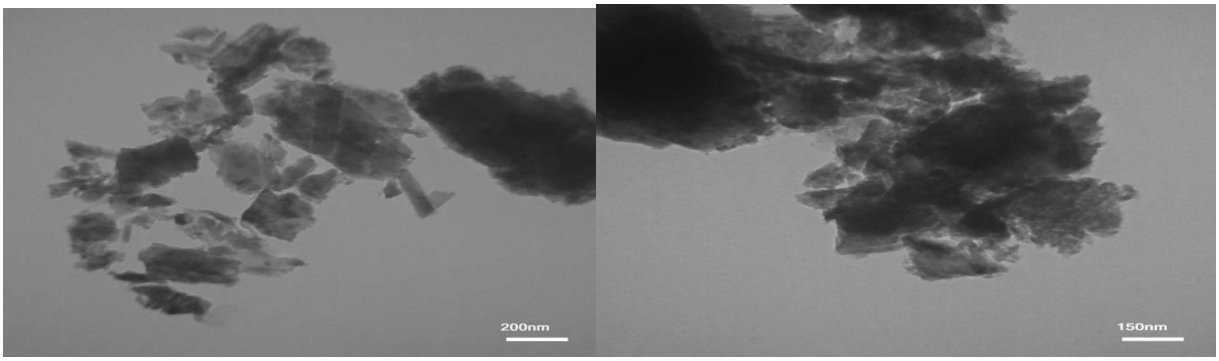

Figure 6. TEM of MnO_2 NPs

2024, 21(3): 0952-0961
https://dx.doi.org/10.21123/bsj.2023.8183
P-ISSN: 2078-8665 - E-ISSN: 2411-7986
Baghdad Science Journal

AFM analysis

AFM surface analysis must be thoroughly examined due to numerous factors, such as deformations or image artifacts resulting from a tip and contamination, which may produce misleading results. The decision to operate in contact or without contact is one of the critical factors. The contact mode, or degree of surface contact, between the sample and its tip, damages MnO_2 NPs severely. The tip is placed very close to the sample but not in contact with it; hence the only mode necessary for this task is the non-contact one. In terms of optical behaviour, Figs. 7 and 8 shows the development of three-dimensional spherical clusters of MnO_2 Nps following metallization. Due to the environmentally friendly synthesis of the nanomaterials, the sample's surface has pores, is highly rough, and tends to have an amorphous shape[11, 12]. The size of the prepared oxide nanoparticles ranges between 15.00 to 50.00 nm, as shown by the Height Accumulation Distribution Report of MnO_2 NPs. This confirms that the manganese oxide made using pomegranate peel extract is a nano oxide[12].

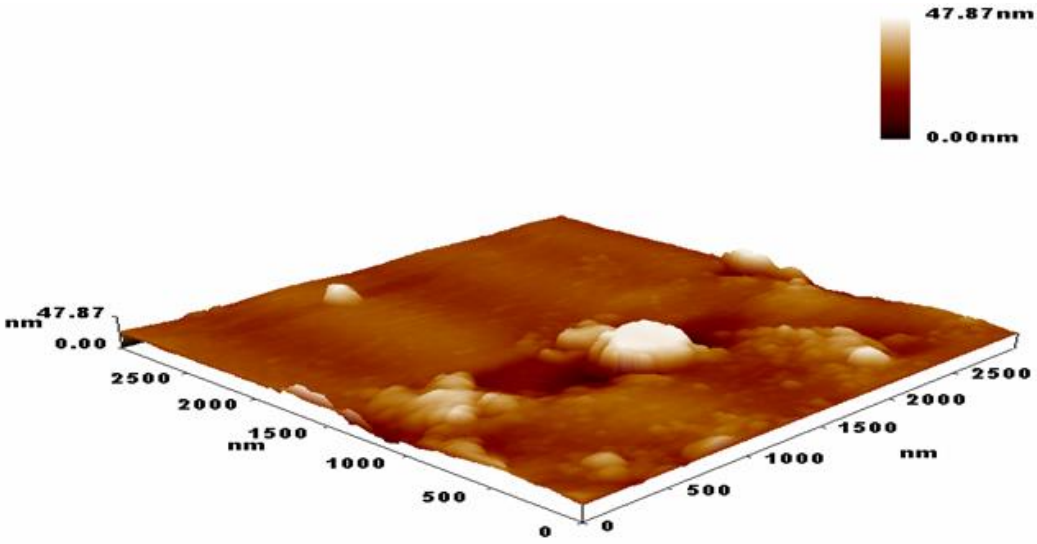

Figure 7. The AFM of MnO_2 NPs.

Height Cumulation Distribution Report

Sample: Sample Name	**Code:**Sample Code
Line No.:lineno	**Grain No.:**2107
Instrument:CSPM	**Date:**2022-09-13
Avg. Height:25.626 nm	**<=10% Height:20.0000 nm**
<=50% Height:25.0000 nm	**<=90% Height:27.5000 nm**

Height(nm) <	Volume(%)	Cumulation(%)	Height(nm) <	Volume(%)	Cumulation(%)	Height(nm) <	Volume(%)	Cumulation(%)
5.0000	0.05	0.05	20.0000	1.57	3.04	35.0000	1.00	96.63
7.5000	0.05	0.09	22.5000	8.59	11.63	37.5000	1.00	97.63
10.0000	0.14	0.24	25.0000	30.99	42.62	40.0000	0.85	98.48
12.5000	0.05	0.28	27.5000	40.58	83.20	42.5000	0.43	98.91
15.0000	0.24	0.52	30.0000	9.35	92.55	45.0000	0.47	99.38
17.5000	0.95	1.47	32.5000	3.08	95.63	47.5000	0.62	100.00

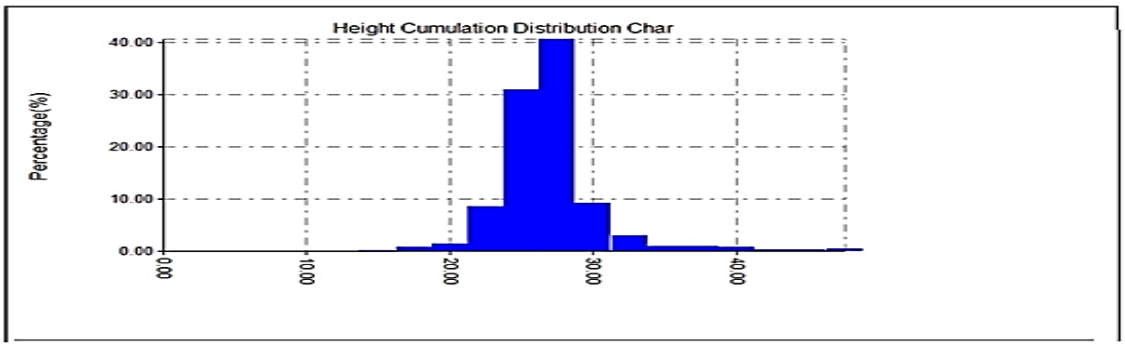

Figure 8. Height Cumulation Distribution Report.

2024, 21(3): 0952-0961
https://dx.doi.org/10.21123/bsj.2023.8183
P-ISSN: 2078-8665 - E-ISSN: 2411-7986
Baghdad Science Journal

Adsorption Study

For each ion, the adsorption time profile was shown in a comparison of the adsorption behaviour of the prepared MnO_2 nanoparticles. The fact that Co (II) exhibits continuous adsorption growth suggests that the process is far from equilibrium and that this is not a straightforward type of adsorption. Instead, it is a precipitation process in which metal oxide nanoparticles act as crystallization nuclei to cause the crystallization of the cobalt chloride salt. The plateau of equilibrium is more distinct for Ni (II) and Cu (II), particularly for Ni (II) Fig. 9. The MnO_2 surface is the largest in an alternate form. This arrangement may be caused by convergences between the atomic radius of the element and that of adsorbate metal ions, which make them easily incorporate with the metal oxide's lattice active sites[13-15].

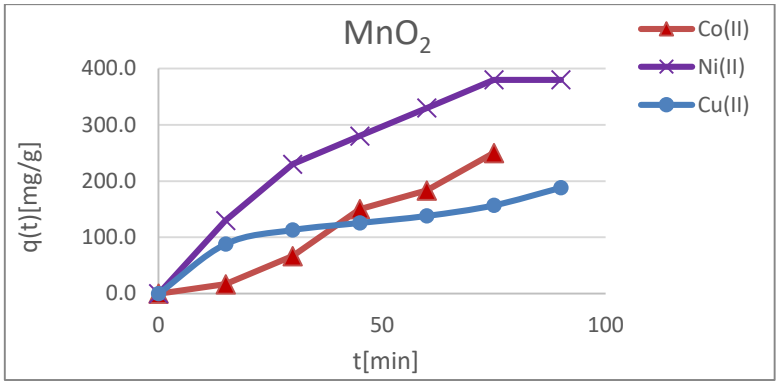

Figure 9. Adsorption time evolution of the metal ions on the MnO_2 surfaces.

The adsorption rate of Ni(II) is the highest in the time scale and conditions of our experiment at all surfaces, whereas Co(II) and Cu(II) ions are close in magnitude, as shown by the above figures. The adsorption process' rate is influenced by (i) charge, (ii) size, and (iii) electronic interactions. Since all ions have the same charge, the first factor (charge) cannot be the leading cause of this difference. Size influences the diffusion process in both the bulk of the solution and the adsorbent mass[16]. According to this theory, Co (II) ought to have the highest adsorption rate, followed by Ni (II) and then Cu (II). However, the observed decrease in the Co (II) adsorption rate and the unrestricted linear growth of the adsorbed portion suggest that there is still another process occurring along with adsorption, which is the Co (II) oxidation by metal oxide[17]; the adsorption percentage of ions on the surface of manganese oxide of mixed Co, Ni, and Cu were 32.79 %, 75.00%, and 30.20%.

Antimicrobial Study

The antibacterial activity of the synthesized MnO_2 nanoparticles was tested using the agar well diffusion method against the bacteria *Escherichia coli*, *Staphylococcus aureus*, and the *Candida fungus* in different concentrations of 25, 50, and 75 mg/L [18,19] and compared with Amoxicillin and Metronidazole as a drug, DMSO solvent medium served as the controls as antibiotics. The antimicrobial activities of the MnO_2 nanoparticles were evaluated by examining the inhibition zone of growth against the used pathogens and adjusting the concentration of the nanoparticles. Table 2, Fig. 10 show the inhibition zone of growth in (mm) of MnO_2 NPs against the bacterial pathogens, two Bactria, and one fungus [20-24].

Table 2.The Inhibition Zone (mm) of MnO_2 NPs against Different Microbial.

Conc.(mg/L)	*Escherichia coli*	*Staphylococcus aureus*	*Candida albicans*
25	5	6	5
50	4	5	4
75	16	12	30

2024, 21(3): 0952-0961
https://dx.doi.org/10.21123/bsj.2023.8183
P-ISSN: 2078-8665 - E-ISSN: 2411-7986
Baghdad Science Journal

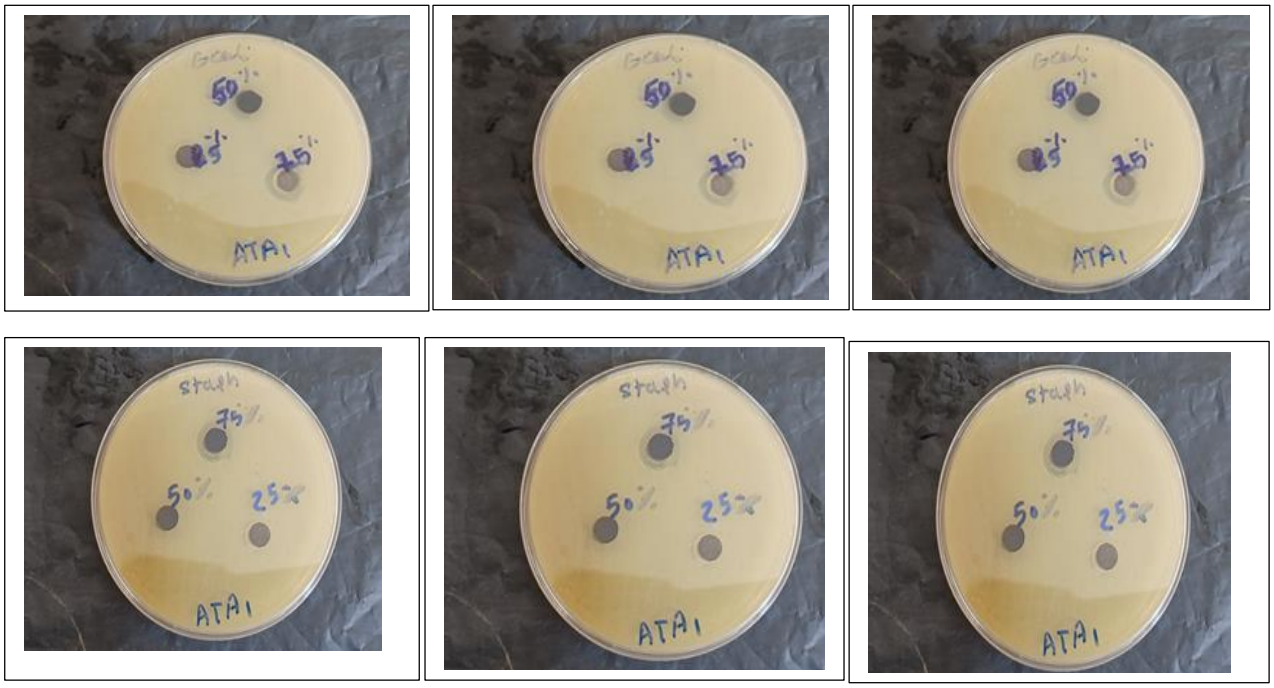

Figure 10. The Inhibition zone of growth.

Conclusion

MnO_2 NPs with a crystal size of 30.94nm were synthesized by a biosynthetic method using Punica Granatum extract and $MnSO_4.H_2O$ salt as starting materials. The product was diagnosed and confirmed to be a nanocomposite by several techniques, including EDX, AFM, SEM, TEM, EDX, UV-vis and IR. It was found that manganese oxide has a thin cluster morphology in its total form. They exhibit antimicrobial activity that significantly slows down bacterial species *Escherichia coli* and *Staphylococcus aureus* growth. As well as antifungals. The adsorption of three metal ions, Co, Ni, and Cu, was also studied at the same time with the removal from water by MnO_2 NPs, i.e. they are percent effective at 32.79 %, 75.00%, and 30.20% in removing salts and heavy elements that are considered water pollutants.

Acknowledgment

The author states their truthful appreciations to Chemistry Department, College of Education for Pure Sciences in Ibn-Al Haitham, University in Baghdad, Iraq for the fiscal support of this study.

Authors' Declaration

- Conflicts of Interest: None.
- We hereby confirm that all the Figures and Tables in the manuscript are ours. Furthermore, any Figures and images, that are not ours, have been included with the necessary permission for re-publication, which is attached to the manuscript.
- Ethical Clearance: The project was approved by the local ethical committee in University of Baghdad.

Authors' Contribution Statement

A. T. A. and L. K. A. K. certify that we have participated title of MS (Biosynthesis, Characterization, Adsorption and Antimicrobial studies of Manganese oxide Nanoparticles Using Punica Granatum Extract) in different roles as follows: Conception, design, acquisition of data,

analysis, interpretation, drafting the MS, revision and proofreading.

References

1. Guerra FD, Attia MF, Whitehead DC, Alexis F. Nanotechnology for environmental remediation: materials and applications. Molecules. 2018 Jul 18; 23(7): 1760. https://doi.org/10.3390/molecules23071760
2. Enrico C. Nanotechnology-based drug delivery of natural compounds and phytochemicals for treating cancer and other diseases. Stud Nat Prod Chem., 2019 Jan 1; 62: 91-123. https://doi.org/10.1016/B978-0-444-64185-4.00003-4.
3. Rheima AM, Khadom AA, Kadhim MM. Removal of Cibacron Blue P-6B dye from aqueous solution using synthesized anatase titanium dioxide nanoparticles: Thermodynamic, kinetic, and theoretical investigations. J Mol Liq., 2022 Jul 1; 357: 119102. https://doi.org/10.1016/j.molliq.2022.119102.
4. Saod WM, Hamid LL, Alaallah NJ, Ramizy A. Biosynthesis and antibacterial activity of manganese oxide nanoparticles prepared by green tea extract. Biotechnol Rep. 2022 Jun 1; 34: e00729. https://doi.org/10.1016/j.btre.2022.e00729.
5. Hoseinpour V, Ghaemi N. Green synthesis of manganese nanoparticles: Applications and future perspective–A review. J Photochem Photobiol B. 2018 Dec 1; 189: 234-43. https://doi.org/10.1016/j.jphotobiol.2018.10.022.
6. Mohammed SH, Rheima A, Al-jaafari F, Al-Marjani MF. Green-synthesis of Platinum Nanoparticles using Olive Leaves Extracts and its Effect on Aspartate Aminotransferase Activity. Egypt J Chem. 2022 Apr 1; 65(4): 1-2. https://doi.org/10.21608/EJCHEM.2021.91747.4355.
7. Yin IX, Zhang J, Zhao IS, Mei ML, Li Q, Chu CH. The antibacterial mechanism of silver nanoparticles and its application in dentistry. Int J Nanomedicine. 2020; 15: 2555. https://doi.org/10.2147/IJN.S246764.
8. Parthiban E, Manivannan N, Ramanibai R, Mathivanan N. Green synthesis of silver-nanoparticles from Annona reticulata leaves aqueous extract and its mosquito larvicidal and anti-microbial activity on human pathogens. Biotechnol Rep. 2019 Mar 1; 21: e00297. https://doi.org/10.1016/j.btre.2018.e00297.
9. Rheima AM. Dye-sensitized Solar Cells Based on Silicon Dioxide Nanoparticles Photochemically Synthesized: A Comparative Study in the Concentration of the Dye-sensitized. J Nanostruct. 2021 Jul 1; 11(3): 609-17. https://doi.org/110.22052/JNS.2021.03.018.
10. Aziz SN, Al Marjani MF, Rheima AM, Al Kadmy IM. Antibacterial, antibiofilm, and antipersister cells formation of green synthesis silver nanoparticles and graphene nanosheets against Klebsiella pneumoniae. Rev Med Microbiol., 2022 Jan 1; 33(1): 56-63. https://doi.org/10.1097/MRM.0000000000000280
11. Hafez AA, Naserzadeh P, Ashtari K, Mortazavian AM, Salimi A. Protection of manganese oxide nanoparticles-induced liver and kidney damage by vitamin D. Regul Toxicol Pharmacol. 2018 Oct 1; 98: 240-4. https://doi.org/10.1016/j.yrtph.2018.08.005.
12. Adnan LA, Alheety NF, Majeed AH, Alheety MA, Akbaş H. Novel organic-inorganic nanohybrids (MnO2 and Ag nanoparticles functionalized 5-methoxy-2-mercaptobenzimidazole): one step synthesis and characterization. Mater Today Proc. 2021 Jan 1; 42: 2700-5. https://doi.org/10.1016/j.matpr.2020.12.707.
13. Rheima AM, Anber AA, Abdullah HI, Ismail AH. Synthesis of alpha-gamma aluminum oxide nanocomposite via Electrochemical Method for Antibacterial Activity. Nano Biomed. Eng. 2021 Jan 1; 13(1): 1-5. https://doi.org/10.5101/nbe.v13i1.p1-5.
14. Reczek L, Michel MM, Trach Y, Siwiec T, Tytkowska-Owerko M. The Kinetics of Manganese Sorption on Ukrainian Tuff and Basalt—Order and Diffusion Models Analysis. Minerals. 2020 Nov 28; 10(12): 1065. https://doi.org/10.3390/min10121065
15. Karimi F, Ayati A, Tanhaei B, Sanati AL, Afshar S, Kardan A, et al. Removal of metal ions using a new magnetic chitosan nano-bio-adsorbent; A powerful approach in water treatment. Environ. Res. 2022 Jan 1; 203: 111753. https://doi.org/10.1016/j.envres.2021.111753
16. Wang B, Zhai Y, Hu T, Niu Q, Li S, Liu X, et al. Green quaternary ammonium nitrogen functionalized mesoporous biochar for sustainable electro-adsorption of perchlorate. J Chem Eng. 2021 Sep 1; 419: 129585. https://doi.org/10.1021/jp301261h.
17. Bashiri H, Shajari A. Theoretical study of fractal-like kinetics of adsorption. Adsorp Sci Technol. 2014 Aug;32(8):623-34. https://doi.org/10.1260/0263-6174.32.8.623
18. Sadiq Khasro F, Mahmood HS. Enhancement of Antibacterial Activity of Face Mask with Gold Nanoparticles. Ibn al-Haitham J Pure Appl Sci. 2022 Jul 20; 35(3): 25-31. https://doi.org/10.30526/35.3.2844
19. Amer AA, Karem LK. Biological Evaluation and Antioxidant Studies of Nio, Pdo and Pt Nanoparticles

2024, 21(3): 0952-0961
https://dx.doi.org/10.21123/bsj.2023.8183
P-ISSN: 2078-8665 - E-ISSN: 2411-7986
Baghdad Science Journal

Synthesized from a New Schiff Base Complexes. Ibn al-Haitham J Pure Appl Sci. 2022; 35(4): 170-182. https://doi.org/10.30526/35.4.2864.
20. Majeed AH, Mohammed LA, Hammoodi OG, Sehgal S, Alheety MA, Saxena KK, et al. A Review on Polyaniline: Synthesis, Properties, Nanocomposites, and Electrochemical Applications. Int J Polym Sci. 2022 Oct 14; 2022. https://doi.org/10.1155/2022/9047554.
21. Mohammed SS, Aziz NM, Abdul Karem LK. Preparation and Diagnostics of Schiff Base Complexes and Thermodynamic Study for Adsorption of Cobalt Complex on Iraqi Attapulgite Clay Surface. Egypt J Chem. 2021 Dec 1; 64(12): 2-3. https://doi.org/10.21608/ejchem.2021.75540.3703.
22. Ali AH, Shakir ZH, Mazher AN, Mazhir SN. Influence of Cold Plasma on Sesame Paste and the Nano Sesame Paste Based on Co-occurrence Matrix. Baghdad Sci J. 2022; 19(4): 855-864 https://doi.org/10.21123/bsj.2022.19.4.0855 .
23. Shanan ZJ, Majed MD, Ali HM. Effect of the Concentration of Copper on the Properties of Copper Sulfide Nanostructure. Baghdad Sci J. 2022;19(1): 0225-. https://doi.org/10.21123/bsj.2022.19.1.0225 .
24. Baqer SR., Alsammarraie AM A, Alias M, Al-Halbosiy MM, Sadiq AS. In Vitro Cytotoxicity Study of Pt Nanoparticles Decorated TiO2 Nanotube Array. Baghdad Sci J. 2020; 17(4): 1169-1169. https://doi.org/10.21123/bsj.2020.17.4.1169

التحضير الحيوي والتشخيص ودراسات الامتزاز ومضاد الميكروبات لجسيمات اوكسيدالمنغنيز النانوية باستخدام مستخلص قشور الرمان

انغام طارق علي، لقاء خالد عبد الكريم

قسم الكيمياء، كلية التربية للعلوم الصرفة (ابن الهيثم)، جامعة بغداد، بغداد، العراق.

الخلاصة

تضمن العمل في هذا البحث تحضير اوكسيد المنغنيز النانوي من مستخلص النباتي لقشور الرمان و كبريتات المنغنيز في وسط قاعدي وشخص بطرق مختلفة مثل ؛ FT-IR ، الأشعة فوق البنفسجية المرئية ، الفحص المجهري للقوة الذرية وحيود الأشعة السينية ، المجهر الإلكتروني النافذ ، مجهر المسح الإلكتروني ، مطيافية الأشعة السينية المشتتة للطاقة. في حيود الأشعة السينية ، تم تحديد حجم البلورة باستخدام معادلة ديباي شيرر ، والتي وُجد أنها 30.94 نانومتر. تم امتصاص أيونات المعادن التالية M(II)= Co و Ni و Cu بنجاح باستخدام MnO_2 NPs ، وأظهرت النتائج أنه يمكن إزالة أيونات المعادن الثلاثة من الماء في وقت واحد, Ni (II) لديه أعلى معدل امتصاص خلال الفترة الزمنية. كانت كفاءة إزالة أيونات Co ، و Ni ، و Cu أيونات 32.79٪ ، 75.00٪ ، 30.20 ٪. تم اختبار جسيمات MnO_2 النانوية ضد نوعين من البكتيريا ونوع واحد من الفطريات بثلاثة تراكيز مختلفة, تمت مقارنة النتائج مع تلك التي تم استخدام المضادات الحيوية مثل أموكسيسيلين وميترونيدازول للمقارنة النتائج.

الكلمات المفتاحية: الامتزاز ، مضادات الميكروبات ، التخليق الحيوي ، أوكسيد المنغنيز, ازالة.